The exact solution of the Riemann problem with non-zero tangential velocities in relativistic hydrodynamics

By José A. Pons[1], José M$^{\underline{\text{a}}}$ Martí[1] and Ewald Müller[2]

[1]Departament d'Astronomia i Astrofísica

Universitat de València, 46100 Burjassot, Spain

[2] Max-Planck-Institut für Astrophysik, Karl-Schwarzschild-Str. 1,

85748 Garching, Germany

(Received 4 August 1999)

We have generalised the *exact* solution of the Riemann problem in special relativistic hydrodynamics (Martí & Müller 1994) for arbitrary tangential flow velocities. The solution is obtained by solving the jump conditions across shocks plus an ordinary differential equation arising from the self-similarity condition along rarefaction waves, in a similar way as in purely normal flow. The dependence of the solution on the tangential velocities is analysed, and the impact of this result on the development of multidimensional relativistic hydrodynamic codes (of Godunov type) is discussed.

---

1. Introduction

The decay of a discontinuity separating two constant initial states (*Riemann problem*) has played a very important role in the development of numerical hydrodynamic codes in classical (Newtonian) hydrodynamics after the pioneering work of Godunov (1959). Nowadays, most modern high-resolution shock-capturing methods (LeVeque 1992) are based on the exact or approximate solution of Riemann problems between adjacent numerical cells and the development of efficient Riemann solvers has become a research field in numerical analysis in its own (see, e.g., the book of Toro 1998).

Riemann solvers began to be introduced in numerical relativistic hydrodynamics at the beginning of the nineties (Martí, Ibáñez & Miralles 1991). Presently, the use of high-resolution shock-capturing methods based on Riemann solvers is considered as the best strategy to solve the equations of relativistic hydrodynamics in nuclear physics (heavy ion collisions) and astrophysics (stellar core collapse, supernova explosions, extragalactic jets, gamma-ray bursts). This fact has caused a rapid development of Riemann solvers for both special and general relativistic hydrodynamics (see, e.g., the reviews by Ibáñez & Martí 1999, Martí & Müller 1999).

In a previous paper (Martí & Müller 1994; Paper I in what follows), we derived the analytical solution of the Riemann problem for an ideal gas in special relativistic hydrodynamics for initial states where the flow is normal to the initial discontinuity. This solution has proven to be a useful for (i) the generation of analytical solutions to test relativistic hydrodynamic codes, and (ii) the development of numerical hydrodynamic codes based on an exact Riemann solver (e.g., Martí & Müller 1996; Wen, Panaitescu & Laguna 1997). Because the solution only holds for flows which are normal to the initial discontinuity, numerical simulations based on the exact Riemann solver of Martí & Müller (1994) are restricted to one-dimensional (1D) flows. Balsara (1994) and Dai & Woodward (1997) have circumvented this restriction at the price of constructing multi-dimensional Godunov schemes using a Riemann solver based on the two-shock approximation where the rarefaction wave is treated as a shock wave.

In the following we derive the exact solution of a Riemann problem for an ideal gas in Minkowski spacetime with arbitrary tangential velocities. The solution can be implemented in multidimensional special relativistic hydrodynamic codes based on directional splitting, because it allows the computation of the numerical fluxes at every zone interface. Furthermore, according to recent work by Pons et al. (1998), who solve the equations of general relativistic hydrodynamics using special relativistic Riemann solvers, this exact solution can also be implemented in general relativistic hydrodynamic codes. The exact solution also allows one to test the accuracy of other approximate Riemann solvers and codes.

In this paper we closely follow the structure and notation used in Paper I, where one can also find the basic references for the theory of relativistic simple waves and shocks, first discussed by Taub (1948). Two key references in the theory of relativistic fluids are the review by Taub (1978) and the book by Anile (1989). The main idea behind the solution of a Riemann problem (defined by two constant initial states, L and R, left and right of their common contact surface) is that the self-similarity of the flow through rarefaction waves and the Rankine-Hugoniot relations across shocks allow one to connect the intermediate states I_* $(I = L, R)$ with their corresponding initial states, I. The analytical solution of the Riemann problem in classical hydrodynamics (see, e.g., Courant and Friedrichs 1948) rests on the fact that the normal velocity in the intermediate states, $v^n_{I_*}$, can be written as a function of the pressure p_{I_*} in that state (and the flow conditions in state I). Thus, once p_{I_*} is known, $v^n_{I_*}$ and all other unknown state quantities of I_* can be calculated. In order to obtain the pressure p_{I_*} one uses the jump conditions across the contact discontinuity, which are given by

$$p_{L*} = p_{R*} (= p_*) \tag{1.1}$$

$$v^n_{L*}(p_*) = v^n_{R*}(p_*). \tag{1.2}$$

Equation (1.2) is an implicit algebraic equation in p_* and can be solved by means of an iterative method. The function $v^n_{I*}(p_*)$ is constructed by using the relations across the corresponding wave connecting the states I and $I*$.

In the case of relativistic hydrodynamics the same procedure can be followed, the major difference with classical hydrodynamics stemming from the role of tangential velocities. While in the classical case the decay of the initial discontinuity does not depend on the tangential velocity (which is constant across shock waves and rarefactions), in relativistic calculations the components of the flow velocity are coupled through the presence of the Lorentz factor in the equations. In addition, the specific enthalpy also couples with the tangential velocities, which becomes important in the thermodynamically ultrarelativistic regime.

The structure of the paper is the following. First, in §2 we present the equations of relativistic hydrodynamics for a perfect fluid in 3 spatial dimensions. In §3 and §4 we summarise the properties of the flow across rarefaction waves and shocks, respectively, and explain how to obtain the pressure and velocities behind the corresponding waves as a function of the state ahead the waves. In §5 we combine the results from the two previous sections to solve the Riemann problem. Finally, in §6 we discuss the implementation of the solution in numerical relativistic hydrodynamics. Throughout the paper we will recover the corresponding purely normal flow expressions whenever it is of interest.

2. The equations of relativistic hydrodynamics

Let J^μ and $T^{\mu\nu}$ ($\mu, \nu = 0, 1, 2, 3$) be the components of the density current and the energy–momentum tensor of a perfect fluid, respectively

$$J^\mu = \rho u^\mu \tag{2.1}$$

$$T^{\mu\nu} = \rho h u^\mu u^\nu + p\eta^{\mu\nu}, \tag{2.2}$$

where ρ denotes the proper rest–mass density, p the pressure, $h = 1 + \epsilon + p/\rho$ the specific enthalpy, ϵ is the specific internal energy and u^μ is the four-velocity of the fluid, satisfying the normalization condition

$$u^\mu u_\mu = -1 \tag{2.3}$$

(throughout this paper, we will use the summation convention over repeated indices and units in which the speed of light is set to unity). In Cartesian coordinates, $x^\mu = (t, x, y, z)$, the Minkowski metric tensor $\eta^{\mu\nu}$ is given by

$$\eta^{\mu\nu} = \mathrm{diag}(-1, 1, 1, 1). \tag{2.4}$$

The evolution of a relativistic fluid is determined by the conservation equation of rest–mass (continuity equation) and energy–momentum

$$J^\mu_{,\mu} = 0\,, \tag{2.5}$$

$$T^{\mu\nu}_{,\mu} = 0 \tag{2.6}$$

where $_{,\mu}$ stands for the partial derivative with respect to coordinate x^μ. The above system is closed by an equation of state (EOS) which we shall assume as given in the form $p = p(\rho, \epsilon)$.

The normalization condition of the velocity (2.3) leads to

$$u^\mu = W(1, v^x, v^y, v^z) \tag{2.7}$$

where W, the Lorentz factor, is

$$W = (1 - v^2)^{-1/2} \tag{2.8}$$

and

$$v^2 = (v^x)^2 + (v^y)^2 + (v^z)^2. \tag{2.9}$$

The equations of relativistic hydrodynamics admit a conservative formulation which has been exploited in the last decade to implement high-resolution shock-capturing methods. In Minkowski space time the equations in this formulation read

$$\mathbf{U}_{,t} + \mathbf{F}^{(i)}_{,i} = 0 \tag{2.10}$$

where $\mathbf{U}$ and $\mathbf{F}^{(i)}(\mathbf{U})$ $(i = 1, 2, 3)$ are, respectively, the vectors of conserved variables and fluxes

$$\mathbf{U} = (D, S^1, S^2, S^3, \tau)^T \tag{2.11}$$

$$\mathbf{F}^{(i)} = (Dv^i, S^1v^i + p\delta^{1i}, S^2v^i + p\delta^{2i}, S^3v^i + p\delta^{3i}, S^i - Dv^i)^T. \tag{2.12}$$

The conserved variables (the rest-mass density, D, the momentum density, S^i, and the energy density τ) are defined in terms of the *primitive variables*,(ρ, v^i, ϵ), according to

$$\begin{aligned} D &= \rho W \\ S^i &= \rho h W^2 v^i \\ \tau &= \rho h W^2 - p - D. \end{aligned} \tag{2.13}$$

In the following we shall restrict our discussion to an ideal gas EOS with constant adiabatic exponent, γ, for which the specific internal energy is given by

$$\varepsilon = \frac{p}{(\gamma - 1)\rho}. \tag{2.14}$$

We denote by c_s the sound speed, defined by

$$hc_s^2 = \left.\frac{\partial p}{\partial \rho}\right|_s \tag{2.15}$$

where s is the specific entropy, which is conserved along fluid lines. For the EOS under consideration the speed of the sound can be written as

$$c_s = \left(\frac{\gamma p}{\rho h}\right)^{1/2}. \tag{2.16}$$

3. Relation between the normal flow velocity and pressure behind relativistic rarefaction waves

Rarefaction waves are simple waves in which the pressure and the density of a fluid element decreases when crossing them. Choosing the surface of discontinuity to be normal to the x-axis, rarefaction waves would be self-similar solutions of the flow equations depending only the combination $\xi = x/t$. Getting rid of all the terms with y and z derivatives in equations (2.10) and substituting the derivatives of x and t in terms of the derivatives of ξ, the system reads

$$(v^x-\xi)\frac{d\rho}{d\xi}+\{\rho W^2 v^x(v^x-\xi)+\rho\}\frac{dv^x}{d\xi}+\rho W^2 v^y(v^x-\xi)\frac{dv^y}{d\xi}+\rho W^2 v^z(v^x-\xi)\frac{dv^z}{d\xi}=0 \quad (3.1)$$

$$\rho h W^2(v^x-\xi)\frac{dv^x}{d\xi}+(1-v^x\xi)\frac{dp}{d\xi}=0 \quad (3.2)$$

$$\rho h W^2(v^x-\xi)\frac{dv^y}{d\xi}-v^y\xi\frac{dp}{d\xi}=0 \quad (3.3)$$

$$\rho h W^2(v^x-\xi)\frac{dv^z}{d\xi}-v^z\xi\frac{dp}{d\xi}=0. \quad (3.4)$$

Equation (3.1) comes from the equation of continuity. The remaining equations come from the momentum conservation. Equations (3.3)–(3.4) reflect the expected result: If the tangential velocities are zero in the chosen state, no tangential flow will develop inside the rarefaction. Finally, instead of considering the conservation of energy, we use the conservation of entropy along fluid lines (following the same reasoning as in Paper I) which provides a relation between $dp/d\xi$, $d\rho/d\xi$ and $dh/d\xi$

$$\frac{dp}{d\xi}=hc_s^2\frac{d\rho}{d\xi}=\rho\frac{dh}{d\xi}. \quad (3.5)$$

Non-trivial similarity solutions exist only if the determinant of system (3.1)-(3.5) vanish. This leads to the condition

$$\xi=\frac{v^x(1-c_s^2)\pm c_s\sqrt{(1-v^2)[1-v^2c_s^2-(v^x)^2(1-c_s^2)]}}{1-v^2c_s^2}, \quad (3.6)$$

the plus and minus sign corresponding to rarefaction waves propagating to the left $\mathcal{R}_{\leftarrow}$

and right $\mathcal{R}_{\rightarrow}$, respectively. It is important to note that the two solutions for ξ correspond to the maximum and minimum eigenvalues of the Jacobian matrix associated to the fluxes $\mathbf{F}^{(x)}(\mathbf{U})$ (Donat et al., 1998), generalizing the result found for a vanishing tangential velocity in Paper I (equation (32)).

After some manipulation, the system (3.1)-(3.5) can be reduced to just one ordinary differential equation (ODE) and two algebraic conditions

$$\rho h W^2 (v^x - \xi) dv^x + (1 - \xi v^x) dp = 0 \tag{3.7}$$

$$hWv^y = \text{constant} \tag{3.8}$$

$$hWv^z = \text{constant}, \tag{3.9}$$

with ξ constrained by (3.6). From equations (3.8) and (3.9) it follows that $v^y/v^z =$ constant, i.e., the tangential velocity does not change direction along rarefaction waves and it is only allowed to change its absolute value. Notice that, in a kinematical sense, the Newtonian limit ($v^i \ll 1$) leads to $W = 1$, but equations (3.8) and (3.9) do not reduce to the classical limit $v^{y,z} =$ constant, because the specific enthalpy still couples the tangential velocities. Thus, even for slow flows, the Riemann solution presented in this paper must be employed for thermodynamically relativistic situations ($h \gg 1$). The same result can be deduced from the Rankine-Hugoniot relations for shock waves (see next section).

Using (3.6) and the definition of the sound speed (2.16), the ODE (3.7) can be rewritten as

$$\frac{dv^x}{dp} = \pm \frac{c_s}{W^2 \gamma p} \frac{1}{\sqrt{1 + g(\xi_\pm, v^x, v^t)}} \tag{3.10}$$

where $v^t = \sqrt{(v^y)^2 + (v^z)^2}$ is the absolute value of the tangential velocity and

$$g(\xi_\pm, v^x, v^t) = \frac{(v^t)^2 (\xi_\pm^2 - 1)}{(1 - \xi_\pm v^x)^2}. \tag{3.11}$$

The sign of $\xi_\pm$ corresponds to the sign chosen in (3.6). In the limit of zero tangential velocities, $v^t = 0$, the constants in (3.8), (3.9) and g are zero and we obtain

$$W^2 dv^x = \pm\frac{c_s}{\gamma p}dp = \pm\frac{c_s}{\rho}d\rho, \tag{3.12}$$

recovering expression (30) in Paper I.

Considering that in a Riemann problem the state ahead of the rarefaction wave is known, the integration of (3.10) allows one to connect the states ahead (a) and behind (b) the rarefaction wave. Moreover, using (3.6), the EOS, and the following relation obtained from the constraint $hWv^t =$ constant,

$$v^t_b = h_a W_a v^t_a \left\{ \frac{1-(v^x_b)^2}{h_b^2 + (h_a W_a v^t_a)^2} \right\}^{1/2}, \tag{3.13}$$

the ODE can be integrated, the solution being only a function of p_b. This can be stated in compact form as

$$v^x_b = \mathcal{R}^a_{\rightleftharpoons}(p_b). \tag{3.14}$$

Function $\mathcal{R}^a_{\rightleftharpoons}(p)$ is shown in figure 1, for different values of the tangential velocity v^t in state a, the various branches of the curves corresponding to rarefaction waves propagating towards or away from a. Rarefaction waves move towards (away from) a, if the pressure inside the rarefaction is smaller (larger) than p_a. In a Riemann problem the state a is ahead of the wave and only those branches corresponding to waves propagating towards a in figure 1 must be considered. Moreover, one can discriminate between waves propagating towards the left and right by taking into account that the initial left (right) state can only be reached by a wave propagating towards the left (right). The presence of a tangential velocity in the limiting state restricts the value of the normal velocity within the rarefaction wave to smaller values as it is clearly seen from figure 1. Once the pressure in the post-wave state has been obtained, the corresponding tangential velocity follows from (3.13) (see lower panel of figure 1).

4. Relation between post-shock flow velocities and pressure for relativistic shock waves.

The Rankine-Hugoniot conditions relate the states on both sides of a shock and are based on the continuity of the mass flux and the energy-momentum flux across shocks. Their relativistic version was first obtained by Taub (1948) (see also Taub 1978 and Königl 1980).

If Σ is a hyper-surface in Minkowski space time across which ρ, u^μ and $T^{\mu\nu}$ are discontinuous, the relativistic Rankine-Hugoniot conditions are given by

$$[\rho u^\mu] n_\mu = 0 \;, \tag{4.1}$$

$$[T^{\mu\nu}] n_\nu = 0 \;, \tag{4.2}$$

where n_μ is the unit normal to Σ, and where we have used the notation

$$[F] = F_a - F_b, \tag{4.3}$$

F_a and F_b being the boundary values of F on the two sides of Σ.

Considering Σ as normal to the x-axis, the unitarity of n_ν allows one to write it as

$$n^\nu = W_s(V_s, 1, 0, 0), \tag{4.4}$$

where V_s is interpreted as the coordinate velocity of the hyper-surface that defines the position of the shock wave and W_s is the Lorentz factor of the shock,

$$W_s = \frac{1}{\sqrt{1 - V_s^2}}. \tag{4.5}$$

Equation (4.1) allows one to introduce the invariant mass flux across the shock

$$j \equiv W_s D_a (V_s - v_a^x) = W_s D_b (V_s - v_b^x). \tag{4.6}$$

According to our definition, j is positive for shocks propagating to the right. Note that our convention differs from that of both Landau & Lifshitz (1987) and Courant & Friedrichs (1948), but is the same as in Paper I.

Next, the Rankine-Hugoniot conditions (4.1), (4.2) can be written in terms of the conserved quantities D, S^j and τ, and of the mass flux as follows

$$[v^x] = -\frac{j}{W_s}\left[\frac{1}{D}\right], \tag{4.7}$$

$$[p] = \frac{j}{W_s}\left[\frac{S^x}{D}\right], \tag{4.8}$$

$$\left[\frac{S^y}{D}\right] = 0, \tag{4.9}$$

$$\left[\frac{S^z}{D}\right] = 0, \tag{4.10}$$

$$[v^x p] = \frac{j}{W_s}\left[\frac{\tau}{D}\right]. \tag{4.11}$$

Equations (4.9) and (4.10) imply that the quantity $hWv^{y,z}$ is constant across a shock wave and, hence, that the orientation of the tangential velocity does not change. The latter result also holds for rarefaction waves (see §3). Equations (4.7), (4.8) and (4.11) are formally identical to the corresponding equations in Paper I (equations (47)-(49)) and can be manipulated in the same way to obtain v_b^x as a function of p_b, j and V_s. Using the relation $S^x = (\tau + p + D)v^x$ and after some algebra, one finds

$$v_b^x = \left(h_a W_a v_a^x + \frac{W_s(p_b - p_a)}{j}\right)\left(h_a W_a + (p_b - p_a)\left(\frac{W_s v_a^x}{j} + \frac{1}{\rho_a W_a}\right)\right)^{-1}. \tag{4.12}$$

This expression looks like that obtained for vanishing tangential velocity, but its presence is hidden within the Lorentz factor in state a, W_a. From (4.9) and (4.10) expressions for v_b^y and v_b^z can be derived

$$v_b^{y,z} = h_a W_a v_a^{y,z}\left[\frac{1-(v_b^x)^2}{h_b^2 + (h_a W_a v_a^{y,z})^2}\right]^{1/2}. \tag{4.13}$$

The final step is to express j and V_s as a function of the post-shock pressure. From the definition of the mass flux we obtain

$$V_s^{\pm} = \frac{\rho_a^2 W_a^2 v_a^x \pm |j| \sqrt{j^2 + \rho_a^2 W_a^2 (1 - v_a^{x\,2})}}{\rho_a^2 W_a^2 + j^2} \tag{4.14}$$

where V_s^+ (V_s^-) corresponds to shocks propagating to the right (left). The Taub adiabat (Thorne 1973), which relates (only) thermodynamic quantities on both sides of the shock, and the EOS can be used to derive the desired expressions. The procedure is exactly the same as in Paper I, but we will repeat it here for completeness.

The Taub adiabat, the relativistic version of the Hugoniot adiabat, is obtained by multiplying (4.2) first by $(hu_\mu)_a$ and subsequently by $(hu_\mu)_b$ and summing up the resulting expressions. After some algebra one finds

$$[h^2] = \left(\frac{h_b}{\rho_b} + \frac{h_a}{\rho_a}\right)[p]. \tag{4.15}$$

Next the post-shock density ρ_b is eliminated by using the relation

$$\rho_b = \frac{\gamma p_b}{(\gamma - 1)(h_b - 1)}, \tag{4.16}$$

which is valid for an ideal gas. Then the Taub adiabat can be rewritten in the form

$$h_b^2 \left(1 + \frac{(\gamma-1)(p_a - p_b)}{\gamma p_b}\right) - \frac{(\gamma-1)(p_a - p_b)}{\gamma p_b} h_b + \frac{h_a (p_a - p_b)}{\rho_a} - h_a^2 = 0\ , \tag{4.17}$$

which is a quadratic equation for the post-shock enthalpy h_b as a function of p_b. One of the two roots is always negative and must be discarded as a physical solution. Next multiplying (4.2) by n_μ and using the definition of the relativistic mass flux (4.6) one obtains

$$j^2 = \frac{-[p]}{[h/\rho]}, \tag{4.18}$$

which after using the EOS to eliminate ρ_b and inserting the physical solution of (4.15) gives the square of the mass flux j^2 as a function of p_b. Using the positive (negative) root of j^2 for shock waves propagating towards the right (left), equation (4.18) allows one to obtain the desired relation between the post-shock normal velocity v_b^x and the post-shock pressure p_b. In a compact way the relation reads

$$v_b^x = \mathcal{S}^{a}_{\rightleftharpoons}(p_b). \tag{4.19}$$

The function $\mathcal{S}^{a}_{\rightleftharpoons}(p)$ is shown in figure 2 for several values of the tangential velocity v^t in state a. Its various branches correspond to shock waves propagating towards or away from a. In order to select the relevant branch of the function $\mathcal{S}^{a}_{\rightleftharpoons}(p)$ (figure 2) the same argumentation as in the case of rarefaction waves can be used (see §3). When v_b^x is known, (4.13) can be used to determine v^y and v^z in the post-shock state.

5. The solution of the Riemann problem with arbitrary tangential velocities.

The decay of an initial discontinuity gives rise, in general, to three elementary nonlinear waves (see, e.g., Landau & Lifshitz 1987). Two of them can be shocks or rarefaction waves, one moving towards the initial left state and the other towards the initial right state. Between them, two new states appear, namely L_* and R_*, separated from each other through the third wave, which is a contact discontinuity moving along with the fluid. Across the contact discontinuity pressure and normal velocity are constant, while the density and the tangential velocity exhibits a jump. Accordingly, the time evolution of a Riemann problem can be represented as:

$$I \;\rightarrow\; L\,\mathcal{W}_{\leftarrow}\,L_*\,\mathcal{C}\,R_*\,\mathcal{W}_{\rightarrow}\,R \tag{5.1}$$

where $\mathcal{W}$ and $\mathcal{C}$ denote a simple wave (shock or rarefaction) and a contact discontinuity, respectively. The arrows ($\leftarrow$ / $\rightarrow$) indicate the direction (left / right) from which fluid elements enter the corresponding wave.

As in the Newtonian case, the compressive character of shock waves (density and pressure rise across the shock) allows us to discriminate between shocks ($\mathcal{S}$) and rarefaction waves ($\mathcal{R}$):

$$\mathcal{W}_{\leftarrow\,(\rightarrow)} = \begin{cases} \mathcal{R}_{\leftarrow\,(\rightarrow)} & , \quad p_b \leq p_a \\ \\ \mathcal{S}_{\leftarrow\,(\rightarrow)} & , \quad p_b > p_a \end{cases} \tag{5.2}$$

where p is the pressure and subscripts a and b denote quantities ahead and behind the wave. For the Riemann problem $a \equiv L(R)$ and $b \equiv L_*(R_*)$ for $\mathcal{W}_{\leftarrow}$ and $\mathcal{W}_{\rightarrow}$, respectively. Thus, the possible types of decay of an initial discontinuity can be reduced to:

$$(a) \;\; I \;\rightarrow\; L\,\mathcal{S}_{\leftarrow}\,L_*\,\mathcal{C}\,R_*\,\mathcal{S}_{\rightarrow}\,R \quad p_L < p_{L*} = p_{R*} > p_R \tag{5.3}$$

$$(b) \;\; I \;\rightarrow\; L\,\mathcal{S}_{\leftarrow}\,L_*\,\mathcal{C}\,R_*\,\mathcal{R}_{\rightarrow}\,R \quad p_L < p_{L*} = p_{R*} \leq p_R \tag{5.4}$$

$$(c) \;\; I \;\rightarrow\; L\,\mathcal{R}_{\leftarrow}\,L_*\,\mathcal{C}\,R_*\,\mathcal{R}_{\rightarrow}\,R \quad p_L \geq p_{L*} = p_{R*} \leq p_R. \tag{5.5}$$

The solution of the Riemann problem consists in finding the intermediate states, L_* and R_*, as well as the positions of the waves separating the four states (which only depend on L, L_*, R_* and R). The functions $\mathcal{W}_{\rightarrow}$ and $\mathcal{W}_{\leftarrow}$ allow one to determine the functions $v^x_{R*}(p)$ and $v^x_{L*}(p)$, respectively. The pressure p_* and the flow velocity v^x_* in the intermediate states are then given by the condition

$$v^x_{R*}(p) = v^x_{L*}(p) = v^x_*. \tag{5.6}$$

When p_* and v^x_* have been obtained the remaining quantities can be computed. The EOS gives the specific internal energy and the remaining state variables of the intermediate state I_* can be calculated using the relations between I_* and the respective initial state I given through the corresponding wave. In particular, the tangential velocities can be calculated from (3.8) - (3.9) for rarefaction waves and from the Rankine-Hugoniot jump conditions (4.9)-(4.10) for shock waves. Notice that the solution of the Riemann problem depends on the modulus of v^t, but not on the direction of the tangential velocity. Figure 3 shows the solution of a particular Riemann problem (Sod 1978) for different values of the tangential velocity $v^y = 0, 0.5, 0.9, 0.99$. The crossing point of any two lines in the upper panel gives the pressure and the normal velocity in the intermediate states. The range of possible solutions in the (p, v^x)–plane is marked by the shaded region. Whereas the pressure in the intermediate state can take any value between p_L and p_R, the normal flow velocity can be arbitrarily close to zero in the case of an extremely relativistic tangential flow. The values of the tangential velocity in the states L_* and R_* are obtained from the value of the corresponding functions at v^x in the lower panel of figure 3.

To study the influence of tangential velocities on the solution a Riemann problem, we have calculated the solution of a standard test involving the propagation of a relativistic blast wave produced by a large jump in the initial pressure distribution (see Martí & Müller 1999) for different combinations of v^t_L and v^t_R. The initial data are $p_L = 10^3$, $\rho_L = 1$, $v^x_L = 0$; $p_R = 10^{-}2$, $\rho_R = 1$, $v^x_R = 0$ and the 9 possible combinations of $v^t_{L,R} = 0, 0.9, 0.99$. The results are given in figure 4 and table 1.

The speeds of the waves propagating to the left and right, respectively, tend to zero in the limit of $v^t_{L,R} \to 1$. This result is easily deduced from (3.6) which gives the velocities of the head (ξ_h) and tail (ξ_t) of the rarefaction wave, and from (4.14) which gives the shock speed (V_s). These three velocities tend to the normal velocity ahead of the wave (v^x_a) when the corresponding tangential velocity (v^t_a) tends to $v^t_{max} = \sqrt{1 - (v^x_a)^2}$.

Although the structure of the solution remains the same (left propagating rarefaction wave, right propagating blast wave) the values in the constant state change by a large amount. The results show (see figure 4 and table 1) that ξ_h remains constant as long as v^t_L is constant. The value of ξ_h only depends on the left state, and decreases with increasing v^t_L. The pressure in the intermediate state, p_*, increases with increasing v^t_R due to the larger effective inertia of the right state (because of the increase of the Lorentz factor of the right state). The velocity of the shock is determined by the competing effects of an

v_L^t	v_R^t	ρ_{L*}	ρ_{R*}	p_*	v_*^x	V_s	ξ_h	ξ_t
0.00	0.00	9.16e−2	1.04e+1	1.86e+1	0.960	0.987	−0.816	+0.668
0.00	0.90	1.51e−1	1.46e+1	4.28e+1	0.913	0.973	−0.816	+0.379
0.00	0.99	2.89e−1	4.36e+1	1.27e+2	0.767	0.927	−0.816	−0.132
0.90	0.00	5.83e−3	3.44e+0	1.89e−1	0.328	0.452	−0.525	+0.308
0.90	0.90	1.49e−2	4.46e+0	9.04e−1	0.319	0.445	−0.525	+0.282
0.90	0.99	5.72e−2	7.83e+0	8.48e+0	0.292	0.484	−0.525	+0.197
0.99	0.00	1.99e−3	1.91e+0	3.16e−2	0.099	0.208	−0.196	+0.096
0.99	0.90	3.80e−3	2.90e+0	9.27e−2	0.098	0.153	−0.196	+0.094
0.99	0.99	1.29e−2	4.29e+0	7.06e−1	0.095	0.140	−0.196	+0.085

TABLE 1. Solution of the relativistic Riemann problem at $t = 0.4$ with initial data $p_L = 10^3$, $\rho_L = 1.0$, $v_L^x = 0.0$, $p_R = 10^{-2}$, $\rho_R = 1.0$ and $v_R^x = 0.0$ for 9 different combinations of tangential velocities in the left (v_L^t) and right (v_R^t) initial state. An ideal EOS with $\gamma = 5/3$ was assumed. The various quantities in the table are: the density in the intermediate state left (ρ_{L*}) and right (ρ_{R*}) of the contact discontinuity, the pressure in the intermediate state (p_*), the flow speed in the intermediate state (v_*^x), the speed of the shock wave (V_s), and the velocities of the head (ξ_h) and tail (ξ_t) of the rarefaction wave.

increased p_* and the larger inertia of the right state. When increasing v_L^t, both p_* and v_*^x become smaller, leading in turn to a smaller velocity of the shock.

6. Conclusions

We have obtained the exact solution of the Riemann problem in special relativistic hydrodynamics with arbitrary tangential velocities. Unlike in Newtonian hydrodynamics, tangential velocities are coupled with the rest of variables through the Lorentz factor, present in all terms in all equations. It strongly affects the solution, especially for ultra-relativistic tangential flows. In addition, the specific enthalpy also acts as a coupling factor and modifies the solution for the tangential velocities in thermodynamically relativistic situations (energy density and pressure comparable to or larger than the proper rest-mass density), rendering the classical solution incorrect in slow flows with very large internal energies.

Our solution has interesting practical applications. First, it can be used to check the different approximate relativistic Riemann solvers developed by various authors in the last decade, and to test multi-dimensional hydrodynamic codes based on directional splitting. Second, it can be used to construct multi-dimensional relativistic Godunov type methods. The latter project is currently in progress and will be reported elsewhere. Finally, using the procedure described by Pons et al. (1998) the exact solution can be used as a building block in a general relativistic hydrodynamic code.

The computational cost of the exact Riemann solver derived above is comparable to the one presented by Martí & Müller (1994) which is valid for purely normal flows. Hence, when our exact Riemann solver is applied to multi-dimensional flow problems, the difference in efficiency with respect to most linearized Riemann solvers is reduced.

This work has been supported by the Spanish DGICYT grant PB97-1432, and by the agreement between the Spanish CSIC and the Max-Planck-Gesellschaft. J.A.P. acknowledges financial support from the Spanish Ministerio de Educación y Ciencia (FPI grant).

REFERENCES

Anile, A. M. 1989, *Relativistic Fluids and Magnetofluids*, Cambridge University Press.

BALSARA, D.S. 1994, Riemann Solver for Relativistic Hydrodynamics, *J. Comput. Phys.*, **114**, 284.

COURANT, R. AND FRIEDRICHS, K. O. 1948, *Supersonic Flows and Shock Waves*, Interscience.

DAI, W. & WOODWARD, P.R. 1997, An Iterative Riemann Solver for Relativistic Hydrodynamics, *SIAM J. Sci. Comput.*, **18**, 982.

DONAT, R., FONT, J.A., IBAÑEZ, J.M. & MARQUINA, A. 1998, A Flux-Split Algorithm Applied to Relativistic Flows, *J. Comput. Phys.*, **146**, 58.

GODUNOV, S. K. 1959, A Finite Difference Method for the Numerical Computation and Discontinuous Solutions of the Equations of Fluid Dynamics, *Mat. Sb.*, **47**, 271.

IBAÑEZ, J.M. & MARTÍ, J.M. 1999, Riemann Solvers in Relativistic Astrophysics, *J. Comput. Appl. Math.*, in press.

KÖNIGL, A. 1980, Relativistic Gas Dynamics in Two Dimensions, *Phys. Fluids.*, **23**, 1083.

LANDAU, L. D. AND LIFSHITZ, E. M. 1987, *Fluid Mechanics (Second Edition)*, Pergamon.

LEVEQUE, R.J. 1992, *Numerical Methods for Conservation Laws (Second Edition)*, Birkhäuser.

MARTÍ, J.M., IBAÑEZ, J.M. & MIRALLES, J.A. 1991 Numerical Relativistic Hydrodynamics: Local Characteristic Approach, *Phys. Rev.*, D43, 3794.

MARTÍ, J.M. & MÜLLER, E. 1994, The Analytical Solution of the Riemann Problem in Relativistic Hydrodynamics, *J. Fluid Mech.*, **258**, 317.

MARTÍ, J.M. & MÜLLER, E. 1996, Extension of the Piecewise Parabolic Method to One-Dimensional Relativistic Hydrodynamics, *J. Comput. Phys.* **123**, 1.

MARTÍ, J.M. & MÜLLER, E. 1999 Numerical Hydrodynamics in Special Relativity, *Living Reviews in General Relativity*, in press; also astro-ph/9906333.

PONS, J.A., FONT, J.A., MARTÍ, J.M., IBAÑEZ, J.M. & MIRALLES, J.A. 1998, General Relativistic Hydrodynamics with Special Relativistic Riemann Solvers, *Astron. Astroph.* **339**, 638.

SOD, G. A. 1978, A Survey of Several Finite Difference Methods for Systems of Nonlinear Hyperbolic Conservation Laws, *J. Comp. Phys.*, **27**, 1.

TAUB, A. H., 1948, Relativistic Rankine-Hugoniot Relations, *Phys. Rev.*, **74**, 328.

TAUB, A. H., 1978, Relativistic Fluid Mechanics, *Ann. Rev. Fluid Mech.*, **10**, 32.

THORNE, K. S. 1973, Relativistic Shocks: The Taub Adiabat, *Astrophys. J.*, **179**, 897.

TORO, E. 1998, *Riemann Solvers*, Springer.

WEN, L., PANAITESCU, A. & LAGUNA, P. 1997, A Shock–Patching Code for Ultra–Relativistic Fluid Flow, *Astrophys. J.*, **486**, 919.

Figure captions

Figure 1: Loci of states which can be connected with a given state a by means of relativistic rarefaction waves propagating to the left ($\mathcal{R}_{\leftarrow}$) and to the right ($\mathcal{R}_{\rightarrow}$) and moving towards or away from a. Upper panel: pressure versus v^x; lower panel: tangential velocity versus v^x. Solutions for different values of the tangential velocity $v^t = 0, 0.5, 0.9, 0.953$ correspond to solid, dashed, dashed-dotted and dotted lines, respectively. The state a is characterized by $p_a = 0.6$, $\rho_a = 1.0$, and $v^x_a = -0.3$. An ideal gas EOS with $\gamma = 5/3$ was assumed.

Figure 2: Loci of states which can be connected with a given state a by means of relativistic shock waves propagating to the left ($\mathcal{S}_{\leftarrow}$) and to the right ($\mathcal{S}_{\rightarrow}$) and moving towards or away from a. Upper panel: pressure versus v^x; lower panel: tangential velocity versus v^x. Solutions for different values of the tangential velocity $v^t = 0, 0.5, 0.8, 0.865$ correspond to solid, dashed, dashed-dotted and dotted lines, respectively. The state a is characterized by $p_a = 0.25$, $\rho_a = 1.0$, and $v^x_a = -0.5$. An ideal gas EOS with $\gamma = 5/3$ was assumed.

Figure 3: Graphical solution in the (p, v^x)–plane (upper panel) and in the (v^t, v^x)–plane (lower panel) of the relativistic Riemann problem with initial data $p_L = 1.0$, $\rho_L = 1.0$, $v^x_L = 0.0$; $p_R = 0.1$, $\rho_R = 0.125$ and $v^x_R = 0.0$ for different values of the tangential velocity $v^t = 0, 0.5, 0.9, 0.999$, represented by solid, dashed, dashed-dotted and dotted lines, respectively. An ideal gas EOS with $\gamma = 1.4$ was assumed. The crossing point of any two lines in the upper panel gives the pressure and the normal velocity in the intermediate states. The value of the tangential velocity in the states L_* and R_* is obtained from the value of the corresponding functions at v^x in the lower panel, and I_0 gives the solution for vanishing tangential velocity. The range of possible solutions is given by the shaded region in the upper panel.

Figure 4: Analytical pressure, density and flow velocity profiles at $t = 0.4$ for the relativistic Riemann problem with initial data $p_L = 10^3$, $\rho_L = 1.0$, $v_L^x = 0.0$; $p_R = 10^{-2}$, $\rho_R = 1.0$ and $v_R^x = 0.0$, varying the values of the tangential velocities. From left to right, $v_R^t = 0, 0.9, 0.99$ and from top to bottom $v_L^t = 0, 0.9, 0.99$. An ideal EOS with $\gamma = 5/3$ was assumed.

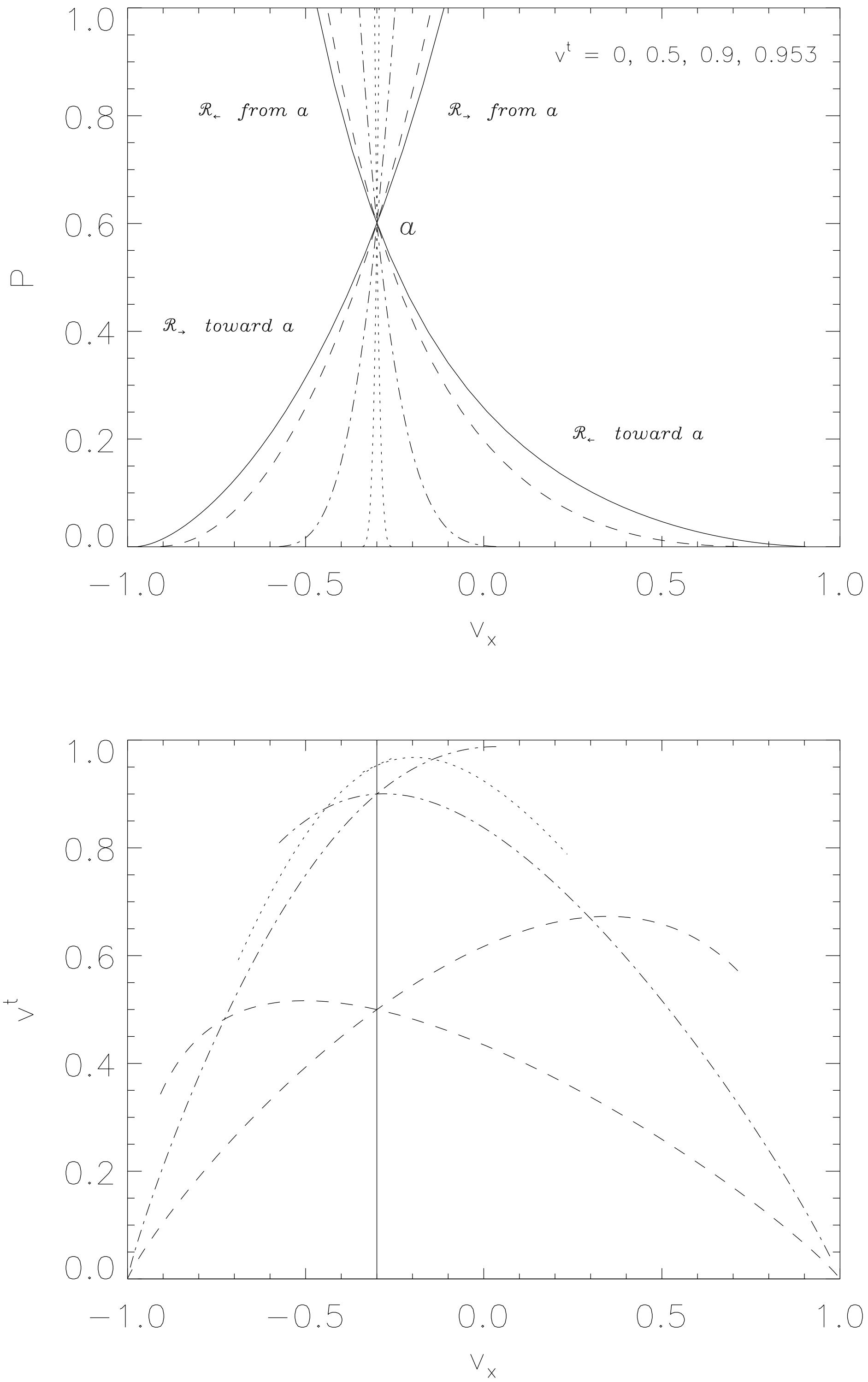

v^t = 0, 0.5, 0.9, 0.953
$\mathcal{R}_{\leftarrow}$ from a
$\mathcal{R}_{\rightarrow}$ from a
a
$\mathcal{R}_{\rightarrow}$ toward a
$\mathcal{R}_{\leftarrow}$ toward a
P
v_x
v^t
v_x

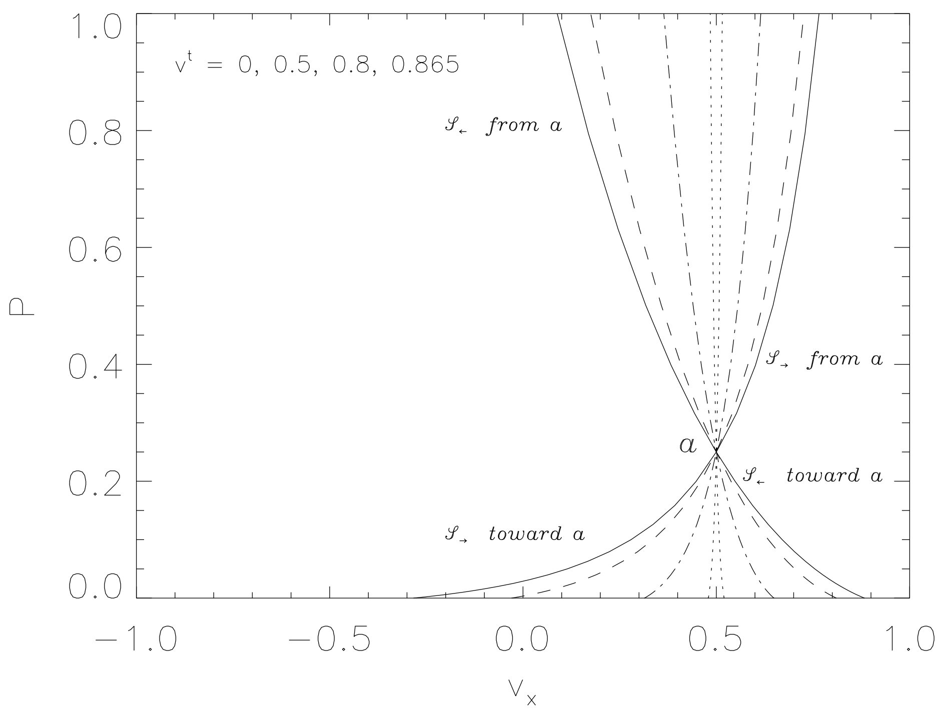
1.0
0.8
0.6
0.4
0.2
0.0
P
−1.0
−0.5
0.0
0.5
1.0
v_x
v^t = 0, 0.5, 0.8, 0.865
$\mathcal{S}_\leftarrow$ from a
$\mathcal{S}_\rightarrow$ from a
a
$\mathcal{S}_\leftarrow$ toward a
$\mathcal{S}_\rightarrow$ toward a

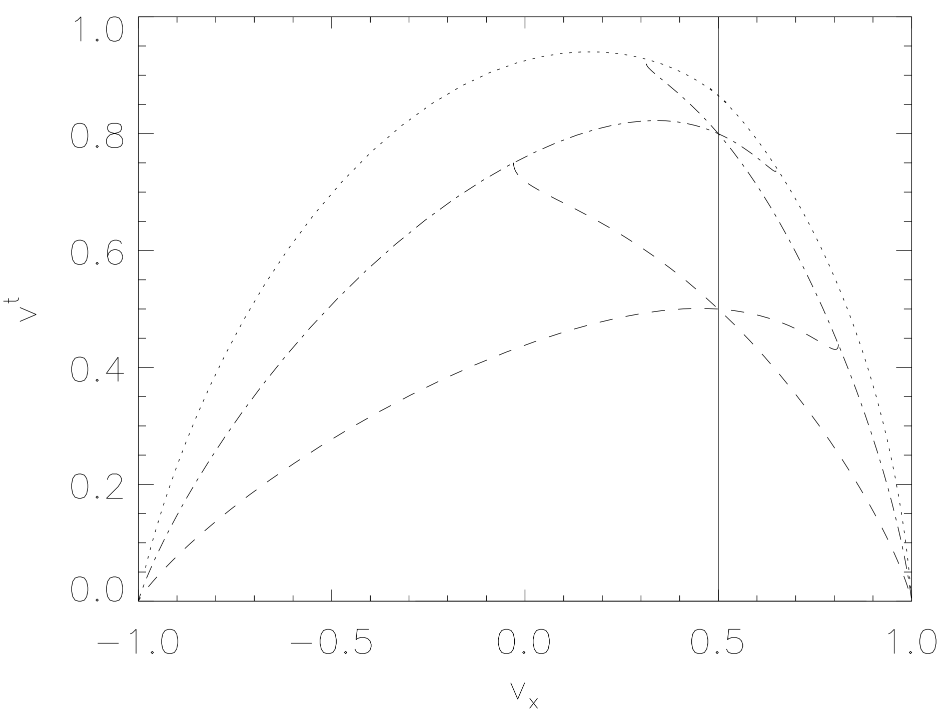
1.0
0.8
0.6
0.4
0.2
0.0
v^t
−1.0
−0.5
0.0
0.5
1.0
v_x

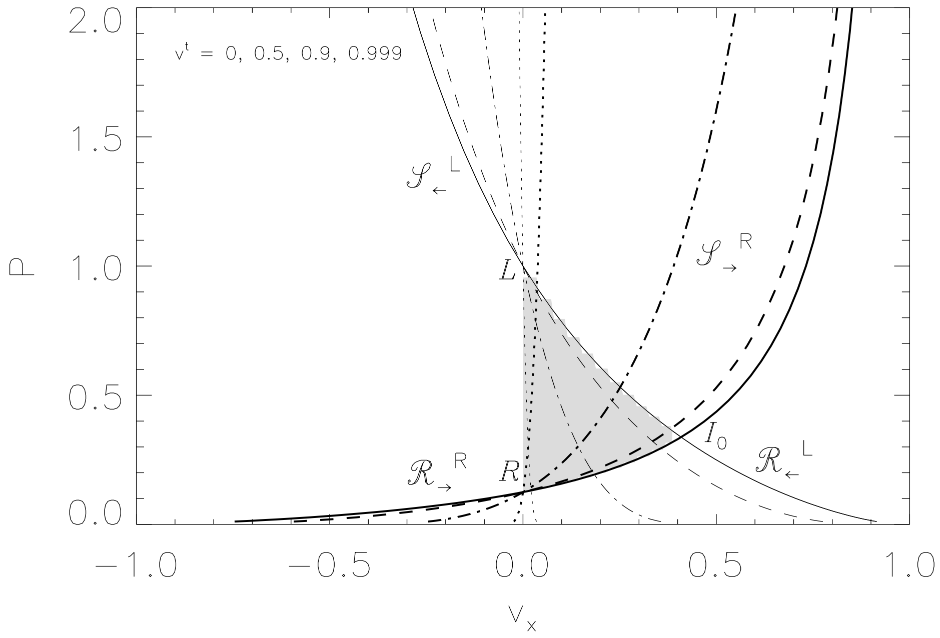

v^t = 0, 0.5, 0.9, 0.999
$\mathcal{S}_{\leftarrow}^{L}$
$\mathcal{S}_{\rightarrow}^{R}$
$\mathcal{R}_{\rightarrow}^{R}$
$\mathcal{R}_{\leftarrow}^{L}$
L
R
I_0
P
V_x

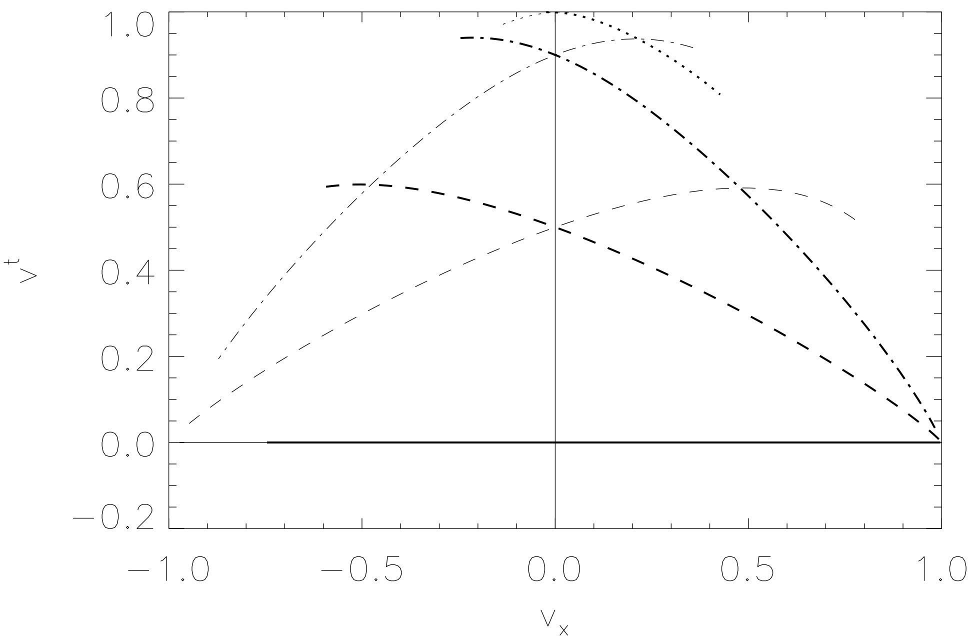

v^t
V_x

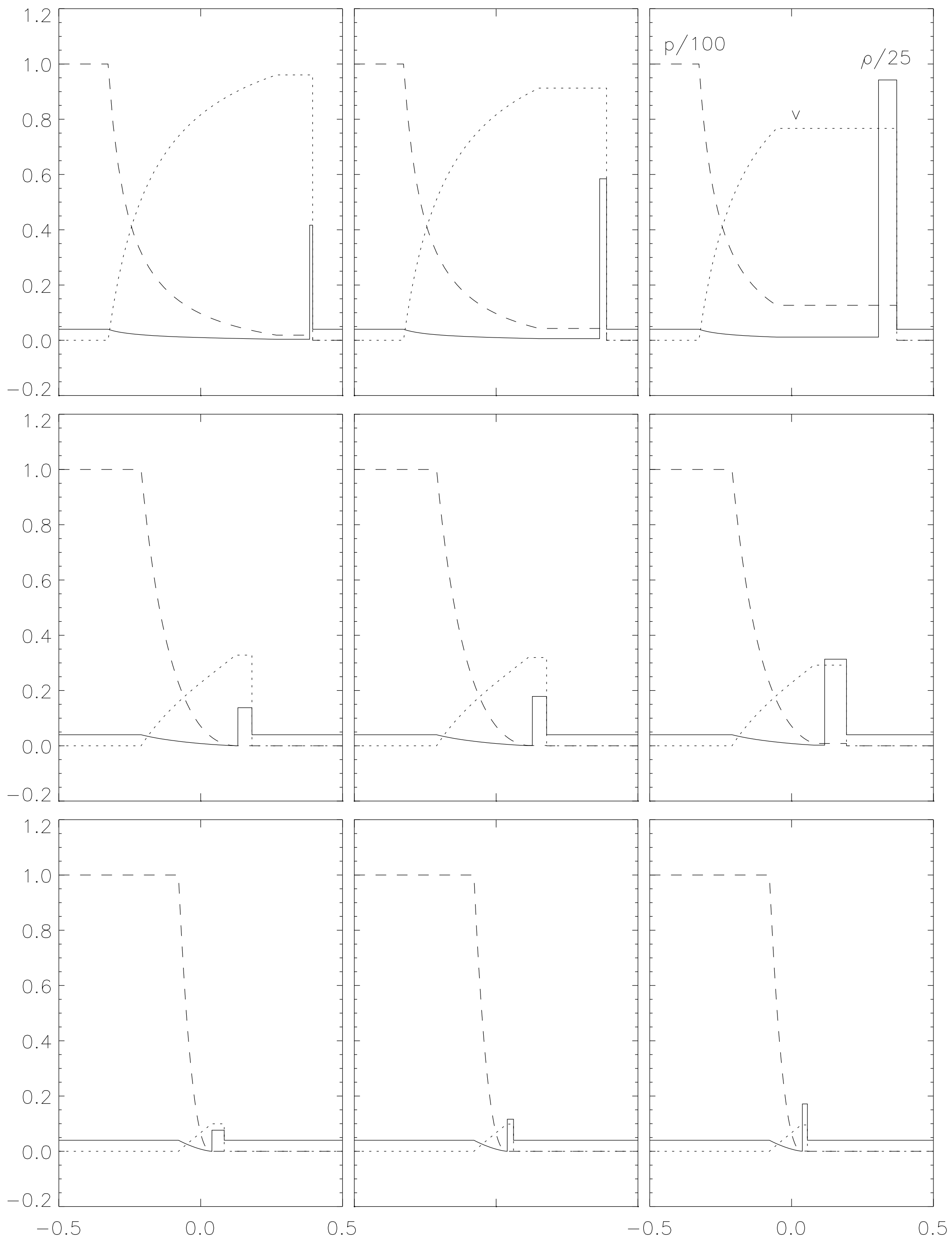

p/100
ρ/25
v
1.2
1.0
0.8
0.6
0.4
0.2
0.0
−0.2
−0.5
0.0
0.5